Cycloreversion performance of coumarin and hetero-coumarin dimers under aerobic conditions: unexpected behavior triggered by UV-A light†

Nikolai Bieniek, [ID] Sebastian Inacker [ID] and Norbert Hampp [ID] *

Photochemical [2+2]-cycloadditions of coumarin-like monomers are the textbook paradigms of photo-formation and photo-cleavage reactions. The electronic conjugation length of monomers and dimers is quite different which results in almost fully separated UV/Vis absorption bands in the UV-A and UV-C. This feature enables the selective light-controlled conversion between monomeric and dimeric forms by the choice of the appropriate wavelengths. Several applications are based on this kind of reversible photo linker without absorption in the visible range. But which is the best molecule from the coumarin family for such an application? Within this study, we compared the photochemical cleavage behavior of twelve coumarin-type cyclobutane dimers. In particular, the influence of isomer structure and substitution pattern was studied. Two dimers with an unexpected high quantum yield for cyclobutane cleavage were identified. This behavior is explained through the differing ring strain of the cyclobutane moiety. Electron donating substitutions of the framework, *e.g.* with a methoxy function (+M-effect), leads to a decreased oxidation potential, making the dimers sensitive towards oxidative dimer splitting. This result disqualifies coumarins, *e.g.* attached to a polymer backbone *via* an ether bond, often in the 7-position, because of their instabilities and side reactions in an aerobic environment. The methylated dimers (+I-effect) show excellent stability towards this undesired side reaction as well as a high cleavage efficiency upon irradiation with 265 nm. All twelve investigated dimers are ranked for their quantum efficiency and rate constant for cleavage at 265 nm, as well as their oxygen tolerance. As the most promising derivative within our scope for applications the methylated coumarin dimer was identified.

Introduction

Light as a tool for chemical transformations offers precise control both on temporal and spatial scales. Desired reaction channels can be addressed by the choice of an appropriate wavelength initiating the formation or the cleavage of bonds within a given molecular framework. Among others, the photochemical [2+2]-cycloaddition, firstly reported for the dimerization of cinnamic acid, is of high interest in organic photochemistry.[1] Today the most prominent structural motif undergoing this reaction is that of coumarin and its derivatives. Upon irradiation with low energy UV-A light (typically above 300 nm), coumarin forms up to four isomeric cyclobutane dimers, only differing in their cyclobutane configuration.[2] The obtained dimeric species show significant differences in their chemical and physical properties

Department of Chemistry, University of Marburg, Hans-Meerwein-Straße 4, D-35032 Marburg, Germany. E-mail: hampp@chemie.uni-marburg.de
† Electronic supplementary information (ESI) available. See DOI: 10.1039/d1cp01919h

compared to the monomeric form. Irradiation of the dimers with high energy UV-C light ($\lambda < 300$ nm) leads to cyclobutane cleavage and the formation of the parent monomeric form.[3] The configuration of the cyclobutane unit, *syn/anti*-head-to-head (hh) or head-to-tail (ht), and the substitutional pattern, influence both cleavage efficiency as well as cleavage kinetics (see Fig. 1).[4,5] The reversible nature of this reaction is utilized in various applications including crosslinking in photoactive polymers,[6] photo-alignment of liquid crystals,[7] or optical data storage,[8] to
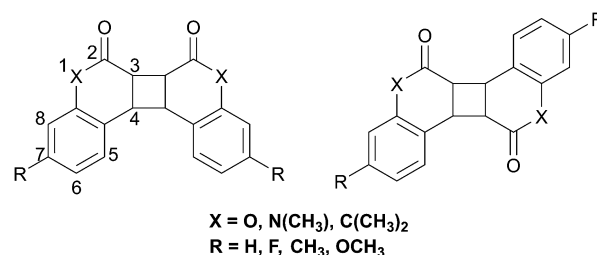

X = O, N(CH$_3$), C(CH$_3$)$_2$
R = H, F, CH$_3$, OCH$_3$

Fig. 1 Schematic structures of the investigated dimers.

This journal is © the Owner Societies 2021

Phys. Chem. Chem. Phys., 2021, **23**, 17703–17712 | 17703

name a few. The broad scope of applications requires fast and efficient photochemical transformations and undesired side reactions should be excluded.

The dimeric forms of coumarin and its derivatives are known to undergo cycloreversion by visible light photocatalysis *via* an oxidative mechanism using *e.g.* flavinium salts or nitrate radicals.[9–12] This oxidative cleavage reaction represents a disadvantage for applications in an aerobic environment, where singlet oxygen can act as an electron acceptor leading to undesired oxidation of organic matter.[13] The redox potential can be tuned by implying electron-withdrawing or -donating groups into the organic framework. The latter reduces this value, making the molecular framework susceptible to oxidation in an aerobic environment.[14]

In our studies, we investigated the relationship between molecular structure and photo- and electrochemical properties employing a substrate scope of twelve dimers derived from the coumarins structural motif. The studied dimers differ in three characteristics as can be seen in Fig. 1. The cyclobutane configuration was altered between head-to-head and head-to-tail isomers and the lactone framework was substituted to the lactam and cyclic ketone analog of coumarin, namely 1-methyl-quinolinone (Q (**5**)) for X = NCH$_3$ and 1,1-dimethyl-naphtalenone (N (**1**)) for X = C(CH$_3$)$_2$. Additionally, electron-withdrawing and donating groups were inserted into the aromatic unit at position 7, as this is the most frequently used position for functionalization. The obtained dimers were investigated towards their cyclobutane cleavage efficiency *via* single photon absorption, their redox potentials as well as their behavior under irradiation with low energy UV-A light ($\lambda > 300$ nm) under aerobic conditions.

Experimental section

Irradiation experiments

For all irradiation experiments in solution, mounted LEDs M265L3 ($\lambda = 265$ nm) or M340L4 ($\lambda = 340$ nm) from Thorlabs with a laboratory power supply were used. The light intensity was determined using a photodiode (S1337-1010BQ, Hamamatsu). All solutions were stirred during irritation. Experiments on long-term stability were carried out in a Rayonet-type batch reactor, which is described in detail in the ESI.†

UV/Vis spectroscopy

UV/Vis spectra were recorded on a Lambda35 (PerkinElmer) photo spectrometer using acetonitrile (Riedel-de-Haën, ≥99.9%) as solvent.

Cyclic voltammetry

The dimer species were studied by cyclic voltammetry in acetonitrile solutions ($c = 3.0$ mM). Tetrabutylammonium hexafluoroborate ($c = 0.1$ M) was added as conducting salt. The electrochemical cell comprised a 3 mm diameter glassy carbon working electrode, a platinum wire counter electrode, and a silver/silver chloride reference electrode (Aldrich). The potentiostat/galvanostat Model 273 A (EG&G Princeton Applied

Research) was used to record the voltammograms. The experiments were carried out at ambient temperature and the solutions were degassed by purging with argon gas. The cyclic voltammograms were recorded in a potential range from -0.5 V to 2.5 V with a scan rate of 100 mV s^{-1}, starting at low potentials. Three cycles were recorded. Data were taken from the second one.

Results and discussion

Dimer synthesis

This study comprises twelve isomer-pure cyclobutane dimers of coumarin and hetero-coumarins (Fig. 2). All dimers were obtained by irradiation of the monomers in a Rayonet-type batch photoreactor with a core wavelength of 350 nm. The detailed experimental procedures for the synthesis of monomers, the dimerization reactions in the batch reactor, as well as the structural analyses and assignments *via* NMR-spectroscopy are presented in the ESI.†

As coumarin is a prominent example for photoinduced [2+2]-cycloadditions in applications, we synthesized and isolated the head-to-head and head-to-tail dimers of four different coumarins, namely parent coumarin hh/ht-C (**1a/b**), 7-methyl-coumarin hh/ht-MeC (**2a/b**), 7-methoxy-coumarin hh/ht-MeOC (**3a/b**) and 7-fluoro-coumarin hh/ht-FC (**4a/b**). Due to the low intersystem crossing yield of the coumarins, the synthesis of the hh-dimers was carried out using benzophenone as a triplet-sensitizer.[15] The head-to-tail dimers were obtained by Lewis-acid catalyzed dimerization.[16] For the synthesis of the
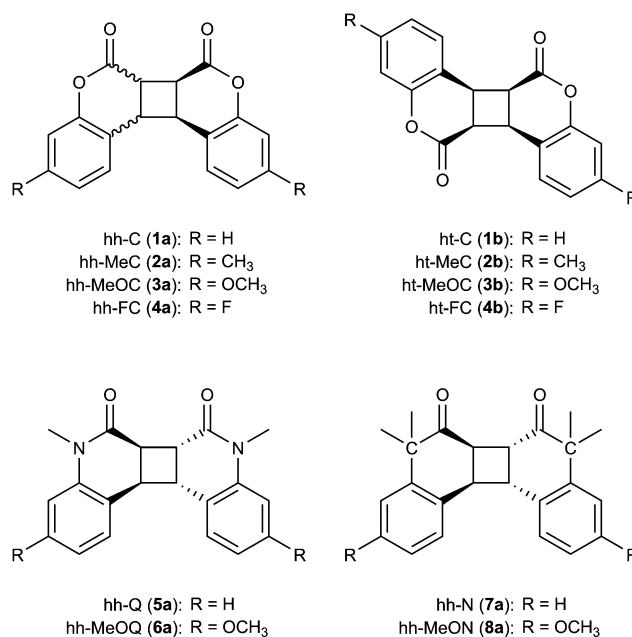

hh-C (**1a**): R = H
hh-MeC (**2a**): R = CH$_3$
hh-MeOC (**3a**): R = OCH$_3$
hh-FC (**4a**): R = F

ht-C (**1b**): R = H
ht-MeC (**2b**): R = CH$_3$
ht-MeOC (**3b**): R = OCH$_3$
ht-FC (**4b**): R = F

hh-Q (**5a**): R = H
hh-MeOQ (**6a**): R = OCH$_3$

hh-N (**7a**): R = H
hh-MeON (**8a**): R = OCH$_3$

Fig. 2 Substrate scope of the investigated dimers. For hh–C (**1a**), hh-MeC (**2a**) the cyclobutane configuration was determined as anti, for hh-MeOC (**3a**) and hh-FC (**4a**) it was determined as syn. The consecutively numbers **1–8** describe the general substitutional pattern, the letters refer to hh (**a**), ht (**b**) or monomeric (**c**) forms.

17704 | *Phys. Chem. Chem. Phys.*, 2021, **23**, 17703–17712

This journal is © the Owner Societies 2021

hetero-coumarin dimers, the monomers were irradiated without an additional triplet-sensitizer. Regarding the head-to-tail structures, no significant amounts of product were received upon dimerization under Lewis-acid conditions, which is in accordance with literature.[17] Thus, we limited the scope to the corresponding head-to-head isomers.

Cyclobutane cleavage with 265 nm irradiation

Upon irradiation with light of a wavelength above 300 nm, the coumarin derivatives undergo [2+2]-cycloaddition as presented in Scheme 1. The obtained cyclobutane dimers cleave back into their parent forms with high energy UV-C light ($\lambda < 280$ nm) (Fig. 3).

The electronic characteristics of the monomeric and dimeric forms alter significantly due to the absence/presence of the double bond in α,β-position of the carbonyl group. Due to the very low absorption of the dimers in the area between 310 nm and 340 nm, the conversion between the two species can be easily traced *via* UV/Vis absorption spectroscopy. The dimer cleavage of hh-C (**1a**), as a representative example, is presented in Fig. 4. Experiments were done in acetonitrile as it does not show nucleophilic behavior, no absorption in the investigated spectral region, and it has high photochemical and electrochemical stability. Using the absorption coefficient at the monomer's absorption maximum above 300 nm, conversions can be expressed in concentrations by Beer–Lambert law as shown in Fig. 5, neglecting the much lower dimer's absorption contribution in the early phase of the reaction. The plots of concentrations *versus* reaction time reveal that the overall cleavage of the head-to-head derivatives is faster than that for the head-to-tail isomers. Functionalization of the aromatic framework with a methoxy group in case of the dimers hh/ht-MeOC (**3a/b**), hh-MeOQ (**6a**), and hh-MeON (**8a**) leads to an enhanced dimer cleavage rate compared to unsubstituted structures. We decided to work on the 7-position functionalization as this is the most common structural motif among a few others for, *e.g.*, linkage to a polymer backbone. The electron-donating effect of this group, and on a smaller scale for the methylated dimers hh/ht-MeC (**2a/b**), leads to enhanced
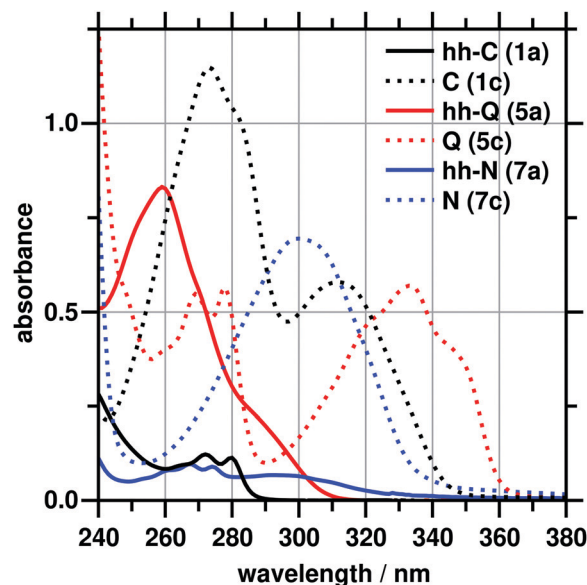
Fig. 3 Absorption spectra for the unsubstituted monomers and dimers of coumarin, quinolinone and napthalenone (0.1 mM in acetonitrile).
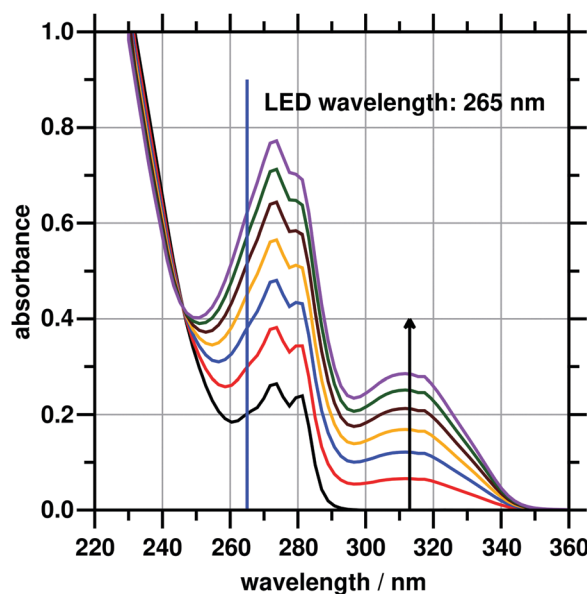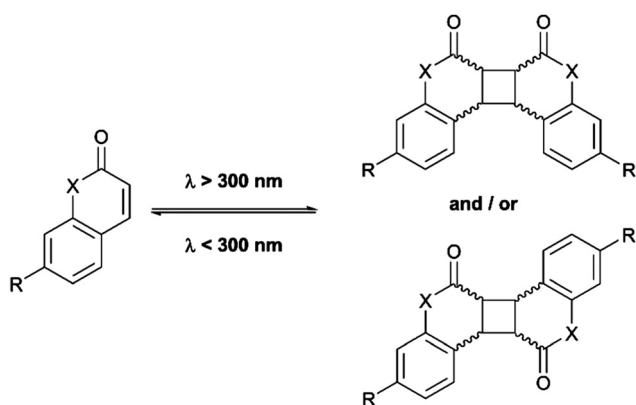
Fig. 4 Formation of monomeric C (**1c**) from hh-C (**1a**) upon irradiation with 265 nm, traced by UV/Vis absorption spectroscopy.

stability of the biradical intermediate during cyclobutane cleavage. Exceptions for this behavior are the dimers hh-Q (**5a**) and hh-MeOQ (**6a**), wherein substitution of the aromatic framework does not lead to an increased cyclobutane cleavage rate. As the influences of the lactam function within these structures dominate the photochemical and photophysical properties of the framework, an additional substitution does not show a significant effect on the cyclobutane cleavage rates.[5] The distinct difference between these two dimers may result from a more efficient back-dimerization of the monomer MeOQ (**6c**) due to its increased electron density arising from the methoxy substitution.

Scheme 1 Photodimerization and photocleavage of the investigated structures.

This journal is © the Owner Societies 2021

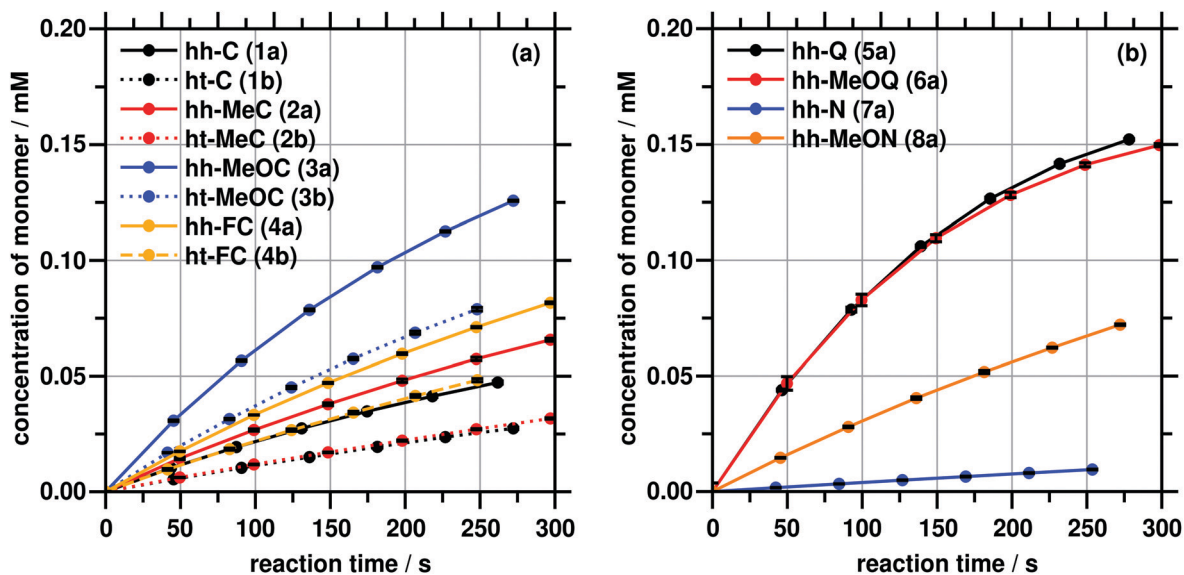*Phys. Chem. Chem. Phys.*, 2021, **23**, 17703–17712 | 17705

Fig. 5 Photoconversion of the dimers to their monomeric forms by irradiation with 265 nm. The lines are added as guides to the eye. (a) coumarin derivatives, (b) quinolinone and naphtalenone with and without methoxy group.

Table 1 Absorption coefficients of dimers ε at 265 nm and 320 nm in acetonitrile, quantum yield Φ for cyclobutane cleavage at 265 nm, obtained rate constant k_0 of zeroth order reaction, and oxidation potentials E_{ox}

	$\varepsilon_{265\ nm}^{ACN}$ [L mol^{-1} cm^{-1}]	$\Phi_{265\ nm}^{SPA}$	k_0 [10^{-6} mol L^{-1} s^{-1}]	$\varepsilon_{320\ nm}^{ACN}$ [L mol^{-1} cm^{-1}]	E_{ox} [V]
hh-C (**1a**)	2028	0.16	0.192	5	2.35
ht-C (**1b**)	1324	0.11	0.105	56	2.27
hh-MeC (**2a**)	2505	0.21	0.234	59	1.94
ht-MeC (**2b**)	1608	0.10	0.110	226	2.20
hh-MeOC (**3a**)	4920	0.23	0.505	107	1.61
ht-MeOC (**3b**)	3047	0.20	0.336	16	2.87
hh-FC (**4a**)	2261	0.26	0.291	33	2.15
ht-FC (**4b**)	2034	0.19	0.202	466	2.33
hh-Q (**5a**)	14 541	0.24	0.737	65	1.53
hh-MeOQ (**6a**)	10 900	0.25	0.706	378	1.20
hh-N (**7a**)	914	0.07	0.038	53	2.30
hh-MeON (**8a**)	1387	0.29	0.277	170	1.47

Only considering the overall conversions from dimeric to monomeric motifs does not reflect the complexity of the photochemical process, as this simple presentation neglects the absorption coefficients of the considered structures at the excitation wavelength of 265 nm. Against this background, we determined the quantum yields Φ_{SPA}, which is defined as the number of cleaved molecules per absorbed photon and deals as a scale for the efficiency of a photochemical process. For the number of cleaved molecules, we considered the initial slope of the plot Δ concentration against reaction time, the reaction volume, and Avogadro's number. The number of photons involved was determined by chemical actinometry utilizing the well-investigated azobenzene *cis/trans*-isomerization and corrected with the corresponding dimer transmission of the reaction solution at 265 nm.[5,18,19] The results are summarized in Table 1. A detailed calculation is found in the ESI.† The results obtained for hh/ht-C (**1**) and hh-Q (**5**) are following previously reported values.[20,21]

The quantum yields for cyclobutane cleavage of the considered coumarin dimers show values between 0.1 and 0.2,

the most efficient cleavage is being achieved with the fluorinated dimer hh-FC (**4a**). The highest quantum yield of all considered dimers was obtained for the dimer hh-MeON (**8a**), but due to its low absorption coefficient at 265 nm, the rate constant for cyclobutane cleavage is rather low. The lowest value is obtained for the DMN dimer hh-N (**7a**).

The plot of the quantum yield *versus* the absorption coefficient at the excitation wavelength 265 nm (Fig. 6) reveals an interesting insight into the relationship between these two factors. Both values show roughly a linear correlation for ε up to about 5000 L mol cm^{-1}. The quantum yields for the dimers hh-Q (**5a**) and hh-MeOQ (**6a**) do not follow this trend but are of the same order of magnitude as for the coumarins. A slightly different cleavage mechanism applies to the lactam dimers.[5] The dimers hh-FC (**4a**) and hh-MeON (**8a**) show the highest quantum yields, but unfortunately only very low absorption coefficients. For those two dimers, a 3D simulation using the PerkinElmer Chem 3D tool reveals a nearly plane cyclobutane surface. For all other considered head-to-head dimers, the

17706 | *Phys. Chem. Chem. Phys.*, 2021, **23**, 17703–17712

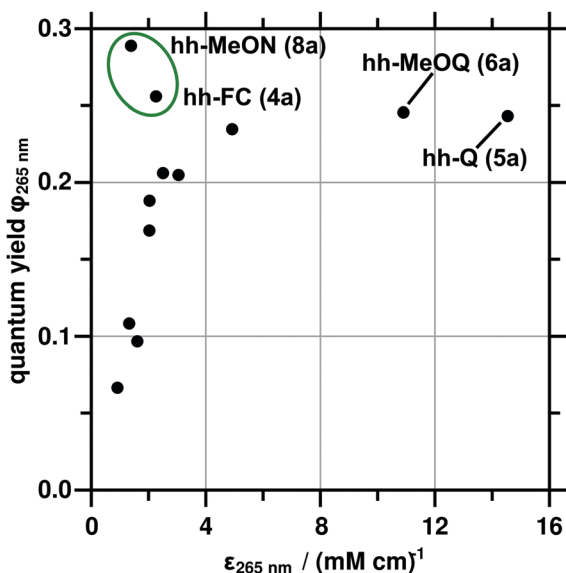This journal is © the Owner Societies 2021

Fig. 6 Relationship between cyclobutane cleavage quantum yield and the absorption coefficient at the excitation wavelength 265 nm.

cyclobutane ring is twisted around 20° thus showing a lower ring tension and in turn higher stability thus cyclobutane cleavage is more unlikely. It is noteworthy that the investigated head-to-tail dimers show smaller torsion angles than the head-to-head derivatives, thus one could expect increased quantum yields for cyclobutane cleavage for these species. We suggest that this behavior is not observed due to the lower stability of the biradicalic intermediate resulting from insufficient mesomeric stabilization close to the carbonyl function. The torsion angles for all investigated structures are given in the ESI.† (Fig. 7)

Cyclic voltammograms of the investigated dimers

The oxidation potentials of the investigated dimers were determined by cyclic voltammetry. The recorded CVs are shown in Fig. 8. All investigated dimers show an irreversible oxidative current at higher potentials independent of configuration or substitution. The dimers hh-C (**1a**), ht-C (**2b**), and hh-N (**7a**) show the highest oxidation potentials of all dimers with values around 2.3 V vs. Ag/AgCl, thus being unlikely to undergo an

oxidative dimer splitting.[9] Due to the electron-rich framework caused by the lactam function of hh-Q (**5a**), the unsubstituted form of this species shows a much lower oxidation potential compared to hh/ht-C (**1a/b**) and hh-N (**7a**). For the integration of coumarins into e.g. a polymer most likely the 7-position is functionalized. Often the polymer network is linked via an oxygen bond. The functionalization of the aromatic unit with a methoxy-function serves as a model and leads to a drastic decrease of the oxidation potential for all three considered species hh/ht-MeOC (**3a/b**), hh-MeOQ (**6a**), and hh-MeON (**8**). This is a serious disadvantage for applications in aerobic environments. It reveals that the functionalization of the coumarin moiety by a CH_3-group, as a model for a system for coumarins covalently bonded into a framework via a C–C linkage, reduces this problem significantly. Due to the missing electron-donating mesomeric effect of this function compared to the ether hh/ht-MeOC (**3a/b**), the oxidation potential should lie in between the methoxy- and the unsubstituted coumarin hh/ht-C (**1a/b**). We determined a value of 1.94 V in the case of the head-to-head dimer hh-MeC (**2a**) and 2.20 V for the head-to-tail species ht-MeC (**2b**). The reduced oxidation probability compared to coumarin can be assigned to the hyperconjugation and thus the weak electron-donating behavior of the CH_3-group. In the case of the fluorinated derivatives hh/ht-FC (**4a/b**), the oxidation potential was expected to be even higher than that of the unsubstituted coumarin dimers due to the strong electron-withdrawing effect of the fluorine atom. The cyclic voltammetry revealed a value similar to hh/ht-C (**1a/b**). This observation can be attributed to the electron-donating mesomeric effect, which neutralizes the electron-withdrawing inductive effect of the fluorine substituent in accordance with the literature.[14,22]

Cyclobutane cleavage upon long-term irradiation with UV-A light

The investigated dimers show only negligible absorption at wavelengths above 300 nm. The measured absorption coefficients at 320 nm are given in Table 1. The fluorescent tubes of the Rayonet-type batch reactor emit light down to approximately 310 nm. We utilized the overlap of dimer absorption and light emission within this region (UV-A) in our experiments. One might expect that all considered dimers are inert against
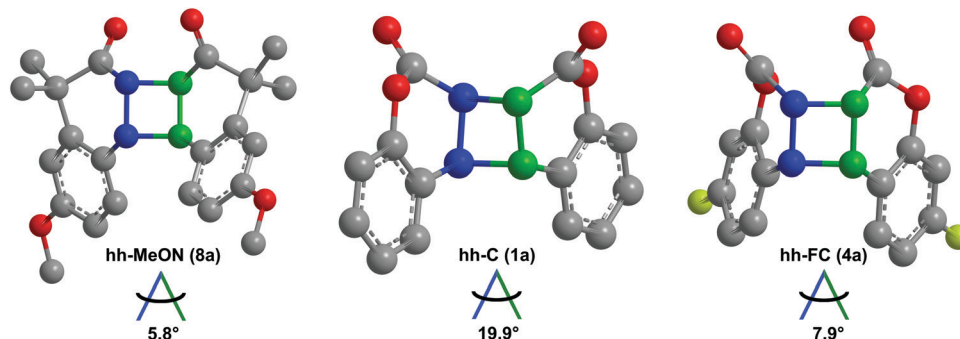

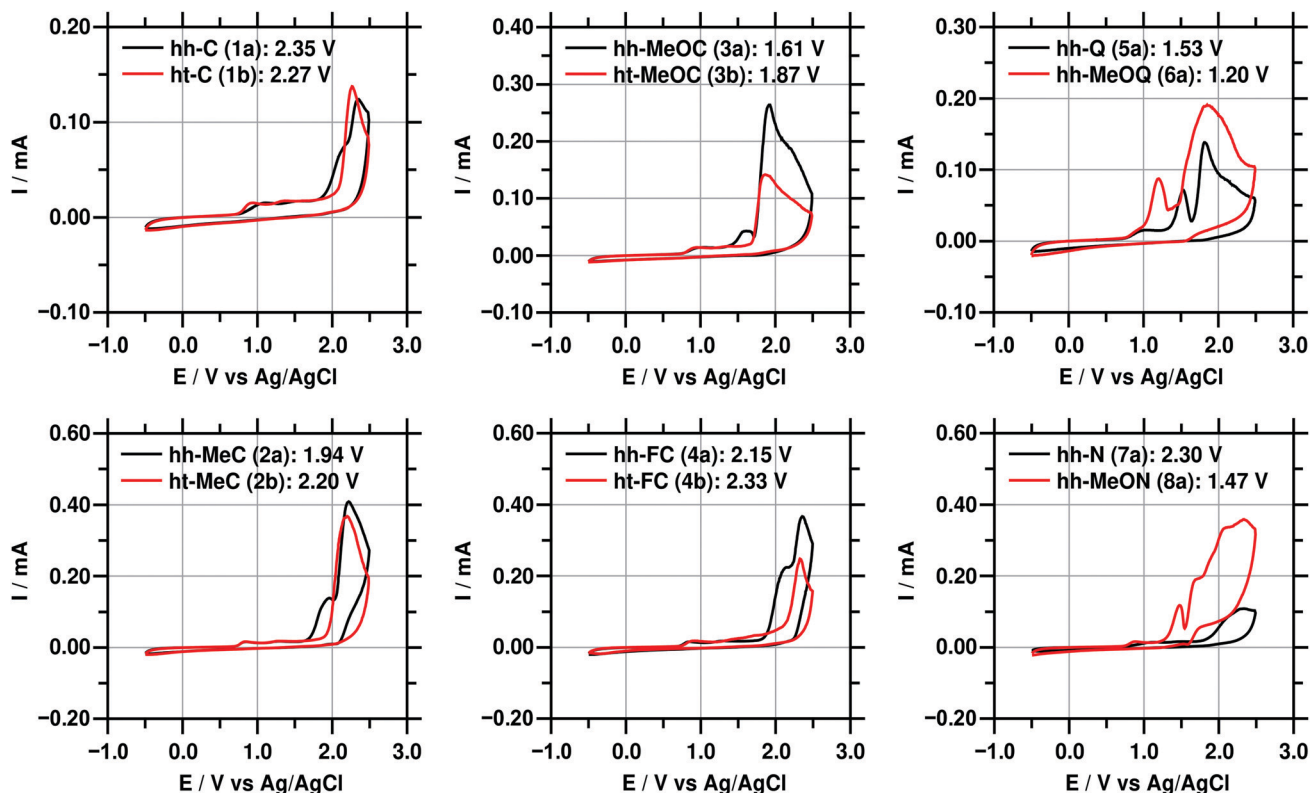Fig. 7 Torsion angles of the cyclobutane moiety for the dimers hh-MeON (**8a**), hh-C (**1a**) and hh-FC (**4a**).

Fig. 8 Cyclic voltammograms of the investigated dimers recorded *versus* an Ag/AgCl reference electrode at 100 mV s^{-1} in acetonitrile. Peak maxima of the oxidation potentials are given in the figures (second cycle is shown, results are summarized in Table 1).

photocleavage in this spectral region, *i.e.* the UV-A regime. However, we found astonishing large deviations from the expected behavior. The experiments were carried out in solutions that were air saturated to simulate an environment away from laboratory conditions. In the case of the coumarins, the efficiencies of singlet oxygen sensitizing have already been studied, especially the methoxy substituted derivatives show potentials towards energy transfer to dissolved oxygen.[23–25] The efficiency of quinolinones regarding energy transfer to oxygen from their excited states producing singlet oxygen was reported just recently.[5] Singlet oxygen acts as an electron acceptor initiating oxidative dimer splitting and leading to the formation of the corresponding monomeric species as well as various amounts of side products, that are not further discussed here. All dimers show a weak absorption in the UV-A-region, thus being potential sensitizers for the formation of singlet oxygen. The reaction products of isomer-pure dimers upon extended irradiation with UV-A light were followed by HPLC. The chromatograms of the methoxy-substituted coumarin dimers hh/ht-MeOC (**3a/b**) after 24 hours of irradiation in the Rayonet-type batch reactor are presented in Fig. 9, as especially this dimer shows an interesting behavior upon irradiation with UV-A light. The recorded chromatograms for all investigated dimers are shown in the ESI.†

The head-to-tail configured dimer ht-MeOC (**3b**) (red trace in Fig. 9) shows only a small degree of conversion to its monomeric form (approx. 3%), whilst the head-to-head dimer hh-MeOC (**3a**) is fully consumed. The monomer MeOC (**3c**) is a
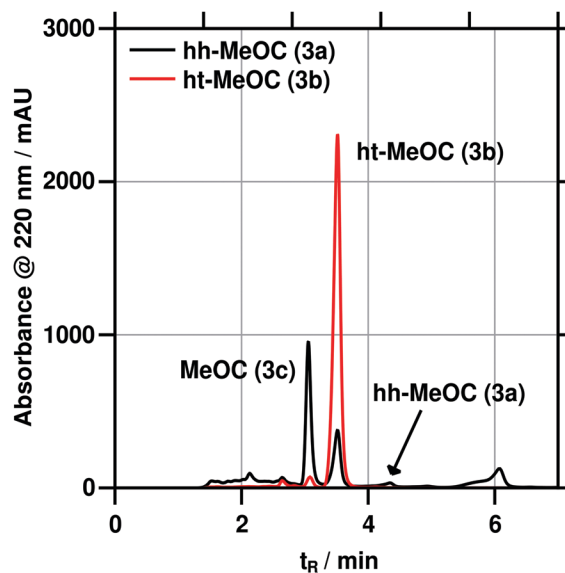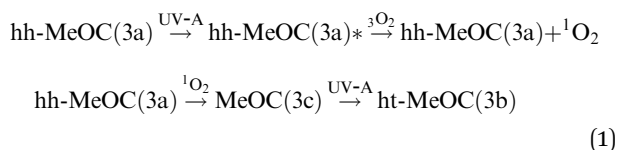

Fig. 9 Chromatograms recorded at 220 nm detection wavelength of the two methoxy-substituted coumarins hh/ht-(**3a/b**) after 24 hours of irradiation with UV-A.

result of the cyclobutane cleavage of hh-MeOC (**3a**). This occurs in such an amount, that the formation of significant amounts of head-to-tail derivative ht-MeOC (**3b**) by photo-dimerization, as well as some side products, are observed. This example

17708 | *Phys. Chem. Chem. Phys.*, 2021, **23**, 17703–17712

This journal is © the Owner Societies 2021

emphasizes the influence of dimer configuration on its stability against external stimuli. In this case, neglecting all side reactions, a head-to-head dimer cleaves into the monomeric form under aerobic conditions which then undergoes cycloaddition into the much more inert head-to-tail isomer. For the description of this reaction sequence, it is worth mentioning that any light in the UV-C region, which is typically needed for the cycloreversion of the hh-MeOC (3a) cyclobutane ring, is excluded. In the first step through the small absorption in UV-A and energy transfer to $^3O_2$, singlet oxygen is generated. This species reacts in the following step with the dimer and causes oxidative cleavage of the cyclobutane ring. The resulting monomers show a high absorption in the UV-A region and dimerization is induced. In this cleavage and dimerization interplay finally, the most stable isomer against singlet oxygen cleavage accumulates.

$$\text{hh-MeOC(3a)} \xrightarrow{\text{UV-A}} \text{hh-MeOC(3a)}* \xrightarrow{^3O_2} \text{hh-MeOC(3a)}+^1O_2$$

$$\text{hh-MeOC(3a)} \xrightarrow{^1O_2} \text{MeOC(3c)} \xrightarrow{\text{UV-A}} \text{ht-MeOC(3b)}$$

$$(1)$$

The resulting distributions of monomeric, dimeric, and unassigned species after extended exposure to UV-A light for the different dimers are presented in Fig. 10. The conversions for the head-to-head dimers with oxidation potentials above 2.0 V (hh-C (1a), hh-FC (4a), and hh-N (7a)) are negligible because they are stable against singlet oxygen. Amongst the other dimers, the methylated coumarin hh-MeC (2a) shows the highest resistance of the head-to-head derivatives against oxidative dimer cleavage with a conversion of about 20% which is due to the comparatively high oxidation potential.
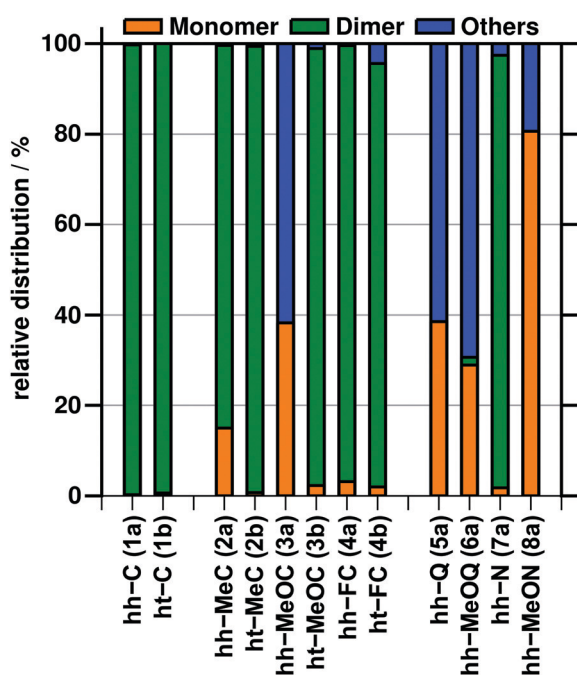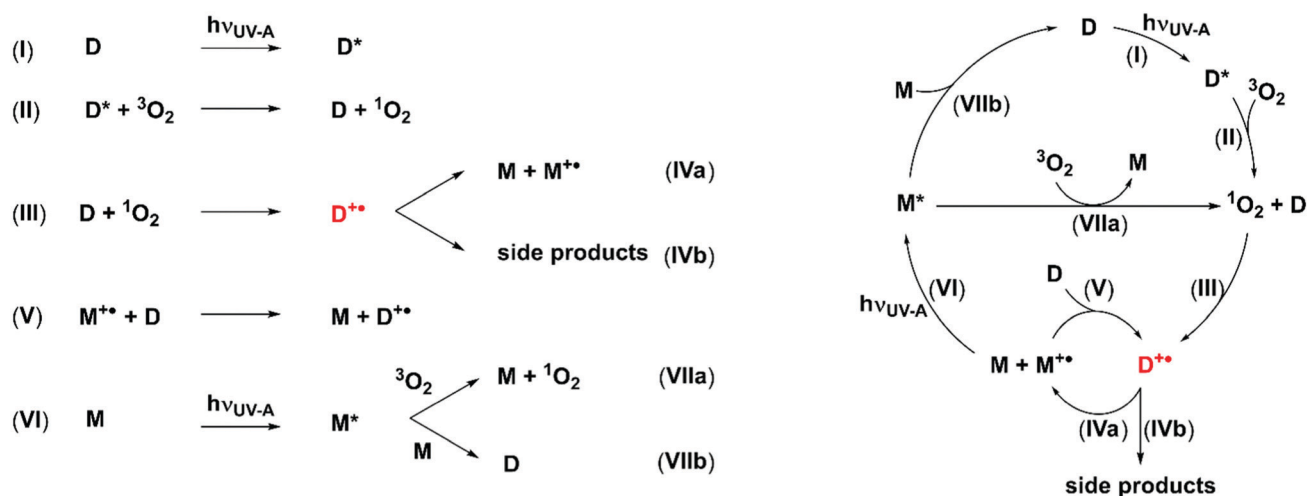

Fig. 10 Distribution between monomeric (orange), dimeric (green), and other species (blue) after 24 hours of irradiation with UV-A in acetonitrile.

All head-to-head dimers show nearly full conversion after 24 hours of irradiation. In contrast, the head-to-tail dimers are all inert against oxidative cyclobutane cleavage, despite their oxidation potentials being similar to their head-to-head analogs.

A mechanistic explanation for this behavior is presented in Scheme 2. The first step (**I**) is the UV-A absorption of the dimer **D**. The efficiency of this process is related to the molar absorption coefficient ε at the used UV-A wavelength. The values for the absorption coefficients at 320 nm are given in Table 1. The excited dimers **D*** transfer their energy to dissolved oxygen (step (**II**)), leading to the formation of the reactive species singlet oxygen $^1O_2$. The previously sensitized singlet oxygen reacts with the dimer in step (**III**) to form the radical cationic form **D$^{+\bullet}$**, which leads to the formation of monomer **M** and the radical cationic monomer **M$^{+\bullet}$** in step (**IVa**) or undesired side products (**IVb**). Those dimers with a high oxidation potential (approx. 1.7 V *vs.* Ag/AgCl) are inert against this oxidation. This step emphasizes the importance of configuration, *i.e.* head-to-head or head-to-tail isomer, independent from the oxidation potential (Fig. 10). For the head-to-head dimers **hh-D$^{+\bullet}$**, the positive charge, as well as the radical, are located at β,β′-position of the carbonyl, being stabilized by the electron-donating effect of the aromatic system. In contrast, the positive charge and the radical are either located at the α-, β-position of the carbonyl or *vice versa* for the ht-dimer (Fig. 11). Due to the electron-poor environment at this position, the intermediate **ht-D$^{+\bullet}$** is not stable and not long-living enough to undergo the following processes.

In step (**V**), the radical cationic form of the monomer **M$^{+\bullet}$** acts as an oxidizing agent for the dimer **D**, leading to the formation of **D$^{+\bullet}$** and **M** again. The formed monomer **M** absorbs UV-A light to form the excited **M*** (**VI**), followed by either dimerization to **D** (step (**VIIb**)) or energy transfer to dissolved oxygen and the formation of singlet oxygen (**VIIa**), which is suitable to oxidize the dimer **D**. Due to the within at least two orders of magnitude higher absorption coefficients in the UV-A (given in the ESI†), the monomers formed during this process lead to an increased concentration of excited molecules and therefore of singlet oxygen. Thus, the reaction proceeds even faster once **M** is formed. We carried out control experiments that demonstrate the influence of singlet-oxygen on cyclobutane cleavage. The results are presented in the ESI.†

In summary, three aspects have to be considered whether a dimer is inert against these processes or not. If the absorption coefficient is rather low, step (**I**) becomes the limiting factor within the mechanism. The efficiencies for singlet oxygen sensitizing are of the same order of magnitude for all investigated dimers, thus step (**II**) should be very similar for those. Step (**III**) is limited by the oxidation potential of the corresponding species. Those showing a high value do not undergo this step, those with a comparably low oxidation potential are oxidized by singlet oxygen and cleaved. Additionally, the configuration of the cyclobutane directs the reaction as the head-to-tail derivatives do not form the crucial stable intermediate **D$^{+\bullet}$**. This mechanism explains the results obtained. The head-to-tail derivatives are inert against oxidative cleavage,

This journal is © the Owner Societies 2021

Phys. Chem. Chem. Phys., 2021, **23**, 17703–17712 | **17709**

Scheme 2 Reaction steps involved in the oxidative cyclobutane splitting with UV-A light.
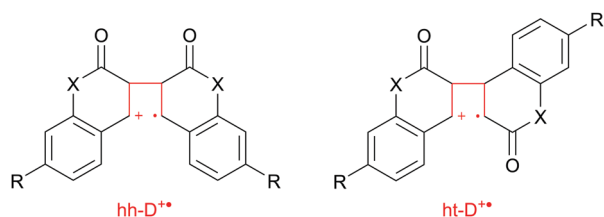

Fig. 11 Difference in radical and charge stabilization for head-to-head and head-to-tail isomers.

as can be derived from the low degrees of conversion towards monomers and side products given in Fig. 10. Despite their rather high absorption coefficients at 320 nm and similar oxidation potentials compared with the head-to-head derivatives, the dimers ht-MeOC (**3b**) and ht-FC (**4b**) show only small degrees of conversion upon irradiation with UV-A. Taking the absorption coefficients in this spectral region as well as the low oxidation potentials for the dimers hh-MeOC (**3a**), hh-Q (**5a**), hh-MeOQ (**6a**), and hh-MeON (**8a**) into account, the almost complete consumption is explained.

Comparison of the dimers regarding stability, rate constant, and quantum yield

To compare the dimers within this substrate scope concerning their stability against irradiation with UV A-light and the induced cyclobutane cleavage *via* oxidation by singlet oxygen, their rate constants and quantum yields for cleavage upon irradiation with 265 nm were normalized and plotted in Fig. 12. As already discussed above, the ht-derivatives within this scope show the lowest probability of undergoing oxidative dimer cleavage. Thus, for applications in an aerobic environment, these isomers are the best choice as they do not undergo the side reaction of oxidative cleavage. The most efficient cleavage upon irradiation with 265 nm was achieved with the methoxy-substituted napthalenone dimer hh-MeON (**8a**). Applications desiring an efficient dimer cleavage, for example, drug release
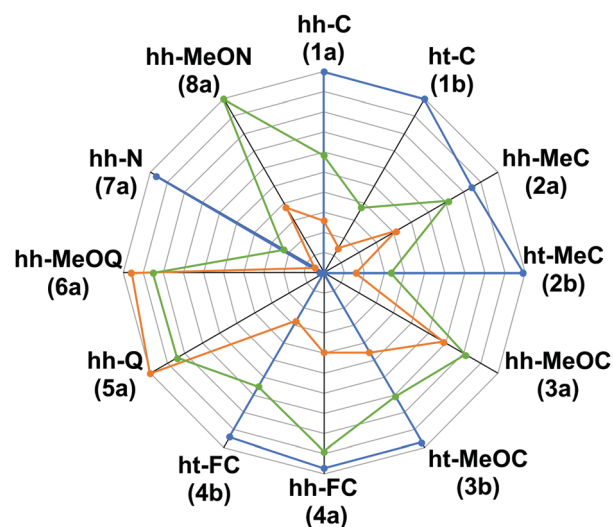

Fig. 12 Normalized comparison of the investigated dimers regarding their stability upon irradiation with UV-A light (blue trace), their rate constants (orange trace) and quantum yield (green trace) for dimer cleavage at 265 nm.

from polymeric materials could experience a boost by implementing this structural motif. The fastest cyclobutane cleavage upon irradiation with 265 nm was achieved with the two quinolinones hh-Q (**5a**) and hh-MeOQ (**6a**). The fast production of monomers within this substance class could be an advantage in applications as medical imaging where a rapid formation and activation of fluorescent probes is desired. As often applications of [2+2]-cycloreversion require high values for all three considered properties, a compromise has to be made. The overall ranking of the considered dimers towards the three properties is given in Fig. 13. The fluorinated derivate hh-FC (**4a**) shows high stability against undesired cleavage upon irradiation with UV A, a high quantum yield, and a moderate rate constant for cleavage at 265 nm. However, further functionalization, which would be necessary to get the fluorinated
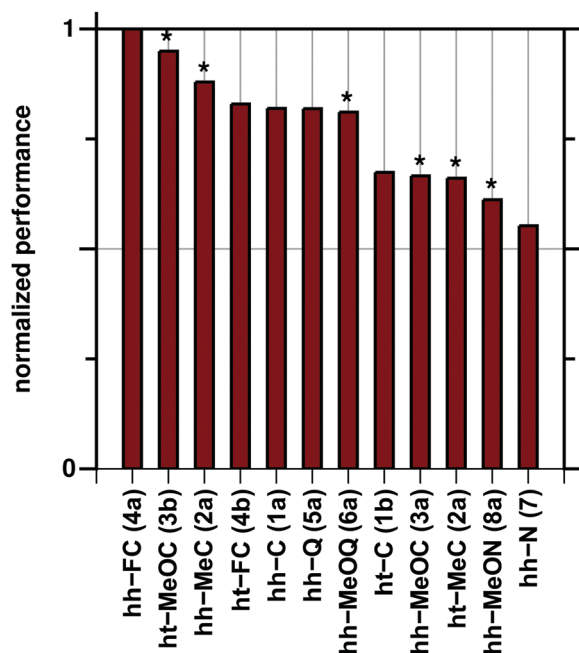
Fig. 13 Normalized performance across the three investigated properties of the dimers within the substrate scope. The dimers capable of being implemented into applications *via* covalent bonding are marked with an asterisk.

coumarin into an application, would affect the here presented and investigated properties of the dimer unpredictably. Substitution *via* ether linking as for ht-MeOC (**3b**) leads to a slight decrease in the dimer's performance. This dimer is suitable for applications that require only one cleavage process, *e.g.* drug release from polymeric materials. However, in aerobic systems which require high reversibility over several dimerization/cleavage cycles, this species should not be considered as the photoactive group. The formation of the unstable hh-MeOC (**3a**) during the dimerization cannot be excluded, which would lead to a loss in performance and activity of the photosystem due to the formation of side products *via* the oxidative dimer cleavage pathway. Thus, the dimer hh-MeC (**2a**) represents the most promising structural motif for applications with repeated dimerization and cleavage. The functionalization with a methyl group can be taken as a model system *e.g.* for covalently bound coumarins in a polymeric matrix *via* C–C-bonding. The moderate quantum yield and cleavage rate constant, as well as the stability against undesired oxidative cyclobutane cleavage, qualify this dimer for applications desiring a fast, efficient, and on the other hand stable photochemical system.

Conclusion

Within this study, the relationship between structure and function of twelve cyclobutane dimers derived from coumarin and its analogs was investigated. A set of eight coumarin dimers with three different functionalizations in the 7-position, each of them as head-to-head and head-to-tail isomer, were synthesized and characterized. In addition, four head-to-head dimers of

hetero-coumarins, also altered in their substitutional pattern were received. The cycloreversion efficiencies upon irradiation with 265 nm, the oxidation potentials of the dimers, and the stability against oxidative cyclobutane cleavage by singlet oxygen were studied. In most cases, a correlation between the quantum yield for 265 nm-induced cleavages and the dimer absorption coefficient at the corresponding wavelength is observed. Two isomers, hh-FC (**4a**) and hh-MeON (**8a**) show an increased photochemical cleavage efficiency. A higher ring tension of the cyclobutane moieties explains this finding. Functionalizations of the dimer framework were used as models for the attachment of the coumarin dimers to a matrix, *e.g.* a polymer. The functionalizations lead to an alteration of the oxidation potentials, *e.g.* implementation of a methoxy function, as a model for an ether-linkage to a polymer backbone, lowers this value efficiently. Methylation was employed as a model for attachment to a polymer backbone by a C–C linkage. The lower the oxidation potential the more the dimers are sensitive to singlet oxygen-triggered cyclobutane cleavage. This is important because all the coumarin monomers and coumarin dimers are sensitizers for singlet oxygen generation with light in the UV-A range which is required for photochemical dimerization. Apart from the oxidation potential, the isomer structure determines whether a cyclobutane ring cleavage occurs or not. Whilst the head-to-head dimers with a comparable low oxidation potential of less than 1.7 V *vs.* Ag/AgCl undergo oxidative cyclobutane cleavage induced by singlet oxygen, the head-to-tail derivatives are inert towards this reaction. This behavior is due to the insufficient stabilization of the radical cationic intermediate. The head-to-head methoxy substituted dimers show the lowest stability against oxidative dimer cleavage which disqualifies these as photoactive structures for applications under aerobic environments. A promising candidate to overcome this problem is the methylated derivative hh-MeC (**2a**). This structural motif can be easily transferred to *e.g.* covalently bonded coumarins in polymers, being a good compromise between cleavage rate, efficiency, and stability against oxidative cleavage.

Financial support

Conflicts of interest

There authors declare no conflict of interest.

Acknowledgements

References

1 C. N. Riiber, *Ber. Dtsch. Chem. Ges.*, 1902, **35**, 2908–2909.
2 C. H. Krauch, S. Farid and G. O. Schenck, *Chem. Ber.*, 1966, **99**, 625–633.

This journal is © the Owner Societies 2021

Phys. Chem. Chem. Phys., 2021, **23**, 17703–17712 | **17711**

3 N. Yonezawa, T. Yoshida and M. Hasegawa, *J. Chem. Soc., Perkin Trans. 1*, 1983, 1083–1086.

4 M. Jiang, N. Paul, N. Bieniek, T. Buckup, N. Hampp and M. Motzkus, *Phys. Chem. Chem. Phys.*, 2017, **19**, 4597–4606.

5 N. Paul, M. Jiang, N. Bieniek, J. L. P. Lustres, Y. Li, N. Wollscheid, T. Buckup, A. Dreuw, N. Hampp and M. Motzkus, *J. Phys. Chem. A*, 2018, **122**, 7587–7597.

6 Y. Chen and J.-L. Geh, *Polymer*, 1996, **37**, 4481–4486.

7 M. Schadt, H. Seiberle and A. Schuster, *Nature*, 1996, **381**, 212–215.

8 K. Iliopoulos, O. Krupka, D. Gindre and M. Sallé, *J. Am. Chem. Soc.*, 2010, **132**, 14343–14345.

9 T. Hartman, M. Reisnerová, J. Chudoba, E. Svobodová, N. Archipowa, R. J. Kutta and R. Cibulka, *ChemPlusChem*, 2021, **86**, 373–386.

10 T. Hartman and R. Cibulka, *Org. Lett.*, 2016, **18**, 3710–3713.

11 O. Krüger and U. Wille, *Org. Lett.*, 2001, **3**, 1455–1458.

12 F. Boussicault, O. Krüger, M. Robert and U. Wille, *Org. Biomol. Chem.*, 2004, **2**, 2742–2750.

13 J. Al-Nu'Airat, M. Altarawneh, X. Gao, P. R. Westmoreland and B. Z. Dlugogorski, *J. Phys. Chem. A*, 2017, **121**, 3199–3206.

14 D. J. Min, K. Lee, H. Park, J. E. Kwon and S. Y. Park, *Molecules*, 2021, **26**, 894.

15 R. Hoffman, P. Wells and H. Morrison, *J. Org. Chem.*, 1971, **36**, 102–108.

16 F. D. Lewis, D. K. Howard and J. D. Oxman, *J. Am. Chem. Soc.*, 1983, **105**, 3344–3345.

17 F. D. Lewis, G. D. Reddy, J. E. Elbert, B. E. Tillberg, J. A. Meltzer and M. Kojima, *J. Org. Chem.*, 1991, **56**, 5311–5318.

18 V. Ladányi, P. Dvořák, J. Al Anshori, Ľ. Vetráková, J. Wirz and D. Heger, *Photochem. Photobiol. Sci.*, 2017, **16**, 1757–1761.

19 H. J. Kuhn, S. E. Braslavsky and R. Schmidt, *Pure Appl. Chem.*, 2004, **76**, 2105–2146.

20 N. Bieniek, S. Inacker, H. Kim and N. Hampp, *J. Photochem. Photobiol., A*, 2021, **414**, 113286.

21 T. Wolff and H. Görner, *J. Photochem. Photobiol., A*, 2010, **209**, 219–223.

22 D. T. Clark, J. N. Murrell and J. M. Tedder, *J. Chem. Soc.*, 1963, 1250.

23 M. Rajendran, J. J. Inbaraj, R. Gandhidasan and R. Murugesan, *J. Photochem. Photobiol., A*, 2006, **182**, 67–74.

24 J. J. Inbaraj, R. Gandhidasan, S. Subramanian and R. Murugesan, *J. Photochem. Photobiol., A*, 1998, **117**, 21–25.

25 T. Wolff and H. Görner, *Phys. Chem. Chem. Phys.*, 2004, **6**, 368–376.